Development Of A Potential Electrode Material For MHD: Yttrium Orthoferrite

Author(s): L. Domingues, T. Negas, A. J. Armstrong, and W. R. Hosle

Session Name: Electrode Wall Materials II

SEAM: 17 (1978)

SEAM EDX URL: https://edx.netl.doe.gov/dataset/seam-17

EDX Paper ID: 762

DEVELOPMENT OF A POTENTIAL ELECTRODE MATERIAL FOR MHD: YTTRIUM ORTHOFERRITE

L. P. Domingues
Trans-Tech, Inc.
Gaithersburg, Maryland 20760

and

T. Negas, A. J. Armstrong and W. R. Hosler
National Bureau of Standards
Washington, D.C. 20234

Abstract

Yttria-based ceramics have not been developed fully for MHD applications. As part of an expanded program, this paper presents some exploratory data related to $YFeO_3$-type materials. Preparation and microchemical/microstructural details together with relevant electrical conductivity and thermal expansion data are given. Emphasis is on $YFeO_3$-$CaFeO_{2.5}$-$CaZrO_3$ solid solutions and composites.

I. Introduction

Perovskites based on mixed rare earth and first row transition metal oxides are remarkable in having diversified magnetic, electrical, and catalytic properties. $LaCrO_3$, "doped" with alkaline earths, has been proposed for "clean-fired" MHD generators since the early work of Meadowcroft[1]. Subsequently, Soviet and French laboratories pursued the development of this material. More recently, researchers at Westinghouse Corp., in cooperation with several other private companies, have made significant advances with $LaCrO_3$-based ceramics prepared by hot-pressing, thermal sintering, and plasma spraying[2]. Researchers at MIT[3] are developing $LaFeO_3$-based materials for slagging MHD generators.

Except for isolated reports from the Soviet Union[4], yttria-based perovskites have been neglected as potentially useful, alternative materials, perhaps, because some are slightly less refractory. However, these ceramics are not susceptible to the destructive mechanical damage due to hydration of excess rare earth oxide sometimes associated with lanthana-based perovskites. This excess may be traced to fabrication methods (e.g. plasma spraying) or to MHD operation (e.g. selective vaporization and/or leaching by seed of the transition metal oxide).

We have initiated an exploratory program to evaluate $YCrO_3$- and $YFeO_3$-based MHD ceramics. Our objectives are to,

a) develope efficient preparation and fabrication methods which yield high density bodies with well-characterized microstructural/microchemical features, and

b) measure pertinent design properties (e.g. electrical/thermal conductivity, thermal expansion).

This paper focuses on $YFeO_3$-based materials having anticipated that associated preparative methods would be less complex than for the more refractory $YCrO_3$ which will be reported later.

II. Experimental Procedures

Yttrium orthoferrite ($YFeO_3$)-based compositions were prepared by direct interaction of intimately mixed oxides of iron, yttrium, and zirconium oxides with calcium carbonate. Ferric (99.5%), yttrium (99.99%), and zirconium (99.8%) oxides were analyzed for volatiles by firing in an alumina crucible at 1300°C for 3 hours. The calcium carbonate was analyzed for calcium oxide and the assay was applied to formulations.

All materials were weighed to an accuracy of ± 0.5 g (>2000 g batches) and mixed thoroughly into a slurry of 50 percent solids. Deionized water was used for all processing. The slurry was dried, granulated, and reacted in air at 1250°C for 6 hours. The resulting samples of the jet milled, calcined material were pressed isostatically at 10,000 psi into bars approximately 3 cm x 1.5 cm x 15 cm. These were fired at 1425°C for 6-8 hours in air. In all cases, pressed specimens were heated and cooled at the rate of 100°C per hour. After this treatment, the density of the bars, as measured by mercury displacement, ranged from 5.19 to 5.48 g/cc which are estimated to be 94-97% of theoretical. Extent of reaction and identity of phases were established by x-ray diffraction and scanning electron microscopic (SEM) analyses of calcined and sintered materials. No attempt was made to optimize the initial reacted powders and sintering conditions for these exploratory specimens.

Electrical conductivity as a function of temperature at various partial pressures of O_2 was measured by the four-probe method. Thermal expansion of selected specimens was measured dilatometrically in air at temperatures up to 1100°C.

III. Results and Discussion

Calcia was added to $YFeO_3$ such that the stoichiometry $Y + Ca/Fe = 1.00$ was maintained. Calcia (a common component, particularly in western coal ashes) was chosen as a "dopant" because the ionic radius of Ca^{2+} more closely approximates that of Y^{3+} and, hence, some substitution for Y is expected. Unfortunately, the pertinent thermochemistry for the system Y_2O_3-CaO-FeO_x is ill-defined. Ideally, under relatively oxidizing conditions, we are dealing with the subsystem $YFeO_3$-$CaFeO_{3-x}$. $YFeO_3$ melts between 1700-1750°C[5] while the $CaFeO_{3-x}$ end-member is typically $Ca_2Fe_2O_5$ ($CaFe^{3+}O_{2.5}$) having the brownmillerite-type structure and a melting point approaching 1450°C[6]. Obviously, the $CaFeO_{3-x}$ component will compromise the refractoriness of $YeFeO_3$, especially if not incorporated into solid solution over a significant compositional range. Furthermore, the low temperature of melting/decomposition (~1100°C) for $Ca_2Fe_2O_5$[7] at low partial pressures of oxygen complicates the thermochemistry. Nevertheless, we prepared several ceramic specimens.

To enhance the refractory nature of $YFeO_3$ (Ca-doped) materials, we explored two compositions containing the refractory perovskite, $CaZrO_3$. Thermochemical features for the subsystem $YFeO_3$-$CaFeO_{2.5}$-$CaZrO_3$ also are not available but must be complicated by the considerations noted above, as well as the phase transitions associated with $CaZrO_3$.

$Y_{1-x}Ca_xFeO_{3-y}$ Ceramics, (x = 0.05, 0.10, 0.15)

The formulation $Y_{1-x}Ca_xFeO_{3-y}$ represents a bulk composition without regard to possible partitioning of elements within a multi-phase ceramic. The undefined parameter y is under investigation but is related to the Ca^{2+} content only when all the Fe is in the 3+ state and the material is an insulator (i.e. $y = x/2$; charge compensation via oxygen vacancies). Figures 1A (900X), 1B (900X), and 1C (900X) illustrate microstructural/microchemical features for compositions with x = 0.05, 0.10, and 0.15, respectively. The dense (ρ = 5.48) $Y_{0.95}Ca_{0.05}FeO_{3-y}$ ceramic is featureless (not etched) and lacks detectable microchemical variation even at higher magnifications. The material clearly is a single-phase solid solution. Ceramics with x = 0.10 (ρ = 5.43) and x = 0.15 (ρ = 5.32) are characterized by a continuous matrix containing irregularly-shaped "islands" of a darker second-phase. Identical phases occur in both compositions as determined by semi-quantitative energy dispersive (EDX) analyses at high magnifications. This suggests that the ceramics were equilibrated (under the imposed sintering conditions) within a two-phase region of the $YFeO_3$-$CaFeO_{2.5}$ system. The matrix phase, dominating the microchemistry, has a composition similar to $Y_{0.95}Ca_{0.05}FeO_{3-y}$ while the second phase appears to be a perovskite solid solution containing the $YFeO_3$ component but richer in the Ca-component. X-ray diffraction powder data confirm these analyses but also reveal significant "broadening" of x-ray lines. Initially, this broadening was attributed to internal prestressing resulting from the two-phase assemblage. However, this hypothesis was precluded when annealed powders yielded similar x-ray patterns. Possible reasons for the line broadening will not be discussed in this paper. Finally, we note that the exact stoichiometry of the Ca-rich, second phase is not yet accurately defined. However, it must be a member within a series which can be formulated as, $Ca_{1-x}Y_xFeO_{2.5+x/2}$. Charge compensation, when all iron is 3+, is accomplished by oxygen vacancies decreasing as the Y-content increases to a maximum, estimated as not exceeding 0.50.

Figures 2A, B, and C illustrate electrical conductivity data for the x = 0.05, 0.10, and 0.15 compositions, respectively. The conductivity of the single-phase material, $Y_{0.95}Ca_{0.5}FeO_{3-y}$,

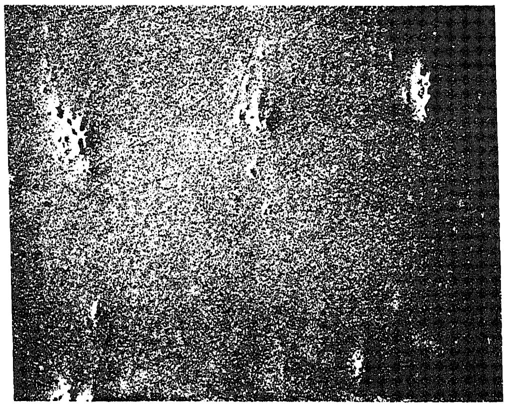

Figure 1A. SEM micrograph (900X) for $Y_{0.95}Ca_{0.05}FeO_{3-y}$ (see text).

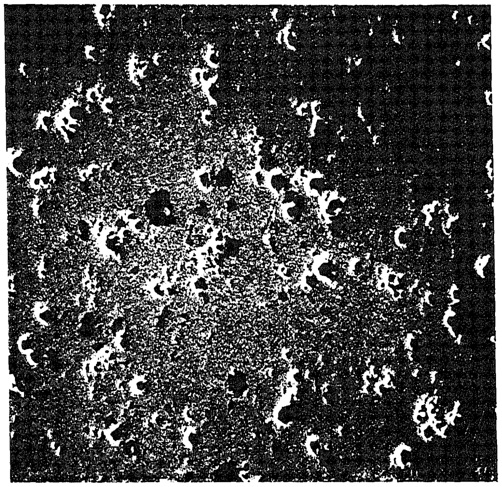

Figure 1B. SEM micrograph (900X) for $Y_{0.90}Ca_{0.10}FeO_{3-y}$ (see text).

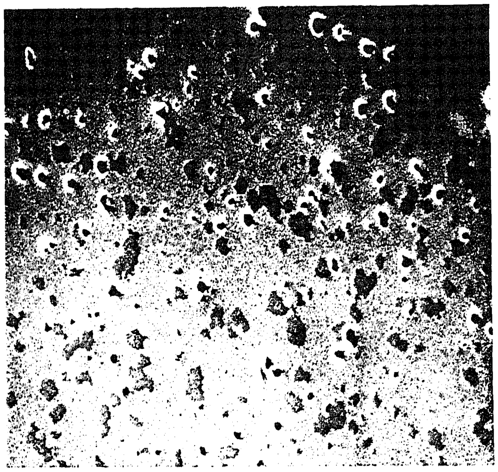

Figure 1C. SEM micrograph (900X) for $Y_{0.85}Ca_{0.15}FeO_{3-y}$ (see text).

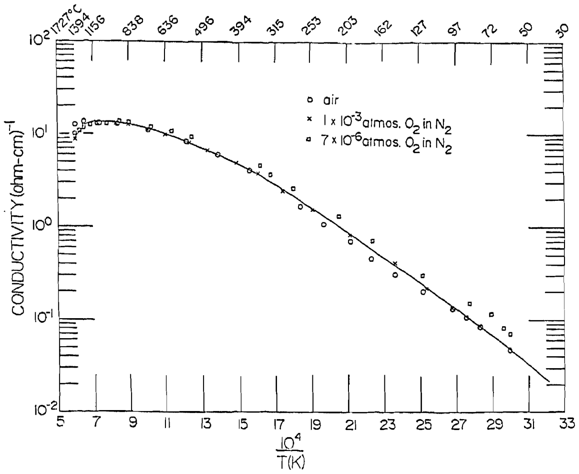

Figure 2A. Electrical conductivity of $Y_{0.95}Ca_{0.05}FeO_{3-y}$.

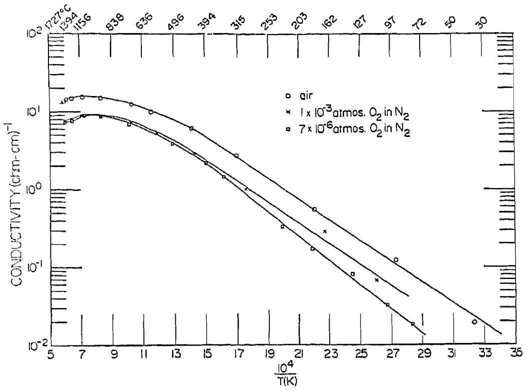

Figure 2B. Electrical conductivity of $Y_{0.90}Ca_{0.10}FeO_{3-y}$.

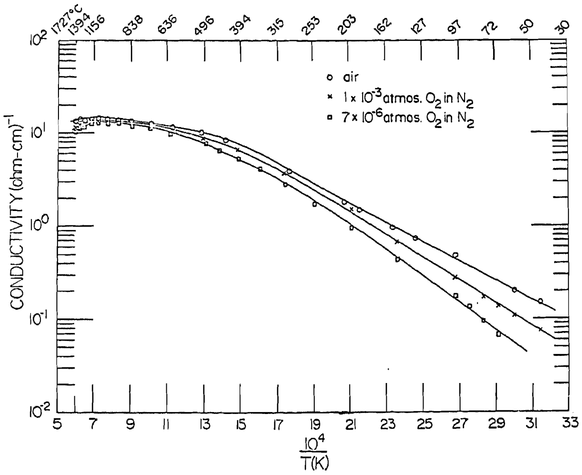

Figure 2C. Electrical conductivity of $Y_{0.85}Ca_{0.15}FeO_{3-y}$.

shows little dependence on P_{O_2} and rivals that of $LaCrO_3$-based ceramics (see Figure 3). Bulk conductivities for the two-phase ceramics, x = 0.10 and 0.15, are similar to this material suggesting that a dominant phase is the primary conductor. This correlates with the microchemistry which consists of a continuous matrix similar in composition to the single-phase material (see above).

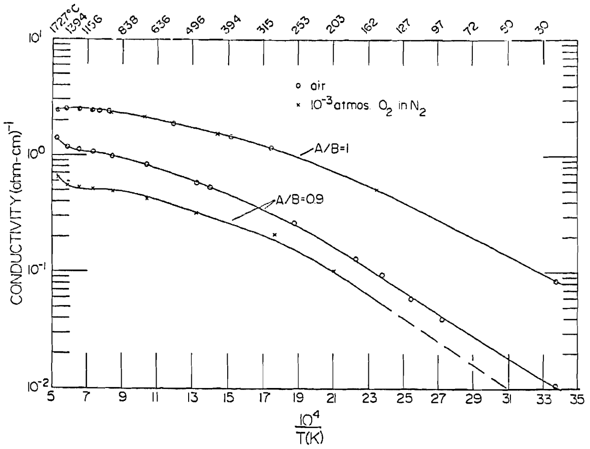

Figure 3. Electrical conductivity of two $LaCrO_3$-based materials. A/B = 1 refers to $La(Mg_{0.02}Cr_{0.98})O_3$ while A/B = 0.9 represents $La_{0.92}Mg_{0.02}CrO_3$. Samples were prepared by H. U. Anderson, A. T. Research Co.

Figure 2A reveals that the electrical conductivity of the single-phase material probably is determined by several competitive mechanisms. Thermoelectric voltages measured at room temperature are consistent with p-type behavior which can be correlated with formulations involving trace quantities of Fe^{4+}. For example, consider the formulation, $Y_{0.95}Ca_{0.05}Fe^{3+}O_{3-y}$. Charge compensation is achieved by the formation of oxygen vacancies according to, $Y_{0.95}Ca_{0.05}Fe^{3+}O_{2.975}$. Simultaneously, trace quantities of Fe^{4+} also are reasonable (see, for example, references 8, 9) to yield, $Y_{0.95}Ca_{0.05}Fe^{3+}_{1-z}Fe^{4+}_{z}O_{2.975+z/2}$. The z - parameter ($Fe^{4+}$-content) is fixed at a maximum of 0.05 for this composition as the bulk oxygen content cannot exceed 3.00. The slight dependence of conductivity on P_{O_2} at the high temperatures may be associated with reduction of Fe^{4+}. This reduction could account for the slight decrease in conductivity observed above $\sim$1200°C. Within the lower temperature regime conductivity appears to be effected by quenching and scattering phenomena.

Figure 4 suggests that the thermal expansion, in air, of $Y_{1-x}Ca_xFeO_{3-y}$ ceramics up to x = 0.15 is not sensitive to bulk composition (see Table 1). This remains consistent with x-ray data which show only slight variation in unit cell parameters for phases observed. Additionally, the two-phase ceramics are not prone to fissuring from fabrication procedures.

Table 1. Summary of Thermal Expansion Data for $YFeO_3$-Based Ceramics.

Material*	Coefficients 20 - 300°C	 300-600°	 600-1100°
A	$10.7 \times 10^{-6}/°C$	11.4	11.8
B	10.8	11.7	12.0
C	10.6	11.3	12.1

* A = $Y_{0.95}Ca_{0.05}FeO_{3-y}$; B = $Y_{0.85}Ca_{0.15}FeO_{3-y}$;

C = $[(Y_{0.85}Ca_{0.15})_{0.80}Ca_{0.20}]\ (Fe_{0.80}Zr_{0.20})O_{3-y}$

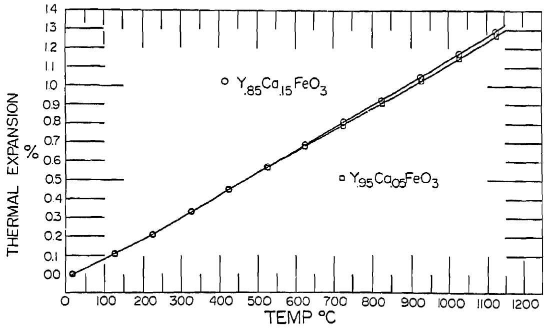

Figure 4. Thermal expansion, in air, for two $YFeO_3$-based materials.

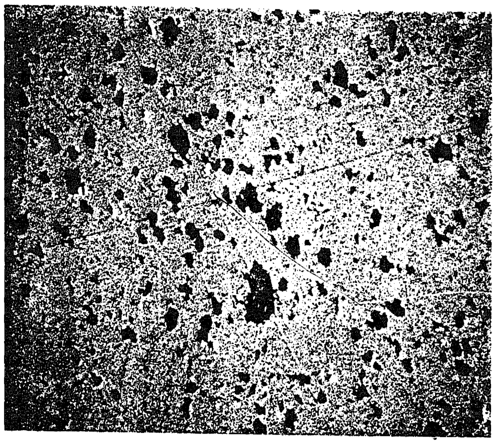

Figure 5. SEM micrograph (900X) of the $[Y_{0.85}Ca_{0.15})_{0.80}Ca_{0.20}]\ Fe_{0.80}Zr_{0.20}O_{3-y}$ material (see text).

$[(Y_{0.85}Ca_{0.15})_{1-x}Ca_x]\ (Fe_{1-x}Zr_x)O_{3-y}$ Ceramics, (x = 0.10, 0.20)

A preliminary base composition $(Y_{0.85}Ca_{0.15})FeO_{3-y}$ was chosen for further reaction with additions of $CaZrO_3$. These are formulated as titled above. The parameter y again is undefined but presumably related to the Ca^{2+} content (see above).

Figure 5 (900X) illustrates microstructural/ microchemical features typical for x = 0.10 ($\rho = 5.29$) and x = 0.20 ($\rho = 5.19$) materials. Both are two-phase mixtures similar to $Y_{1-x}Ca_xFeO_{3-y}$, x = 0.10, 0.15 (see above). The brighter matrix is rich in the $YFeO_3$ component while the darker secondary phase is rich in the "$CaFeO_{2.5}$" component. Although the $CaZrO_3$ component enters into solid solution in both phases, a greater concentration is found within the brighter matrix. These observations indicate that the two-phase field in the $YFeO_3$-$CaFeO_{2.5}$ system extends into the $YFeO_3$-$CaFeO_{2.5}$-$CaZrO_3$ system to, at least, 20 mol % $CaZrO_3$ (under sintering conditions imposed). Single-phase ceramics, if desired, would be predicted when limited concentrations of $CaZrO_3$ are reacted with a base composition such as $Y_{0.95}Ca_{0.05}FeO_{3-y}$.

Electrical conductivity data for compositions at x = 0.10 and 0.20 are shown in Figures 6A and 6B. The anomalous behavior at temperatures above ~1200°C remains unclear. Bulk conductivity, while high, decreases as the insulating component $CaZrO_3$ is incorporated and partitioned between coexisting phases.

Thermal expansion was measured for the x = 0.20 material in air. Data practically coincide with the expansion for $Y_{1-x}Ca_xFeO_{3-y}$, Figure 4, indicating little dependence on bulk composition (see Table 1).

IV. Conclusions

Based on our preliminary studies, $YFeO_3$-based ceramics investigated thus far display desirable features which include,

a) fabrication of dense bodies via thermal sintering at relatively low temperatures without special control of P_{O_2} is relatively simple and this suggests

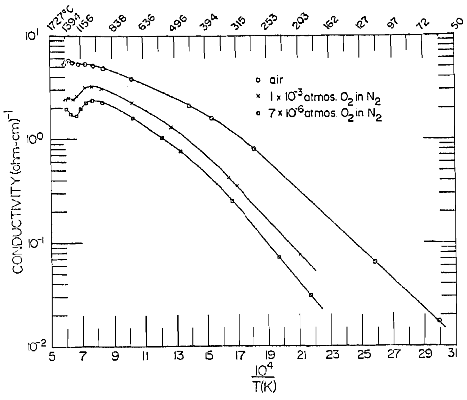

Figure 6A. Electrical conductivity for $[(Y_{0.85}Ca_{0.15})_{1-x}Ca_x]\ Fe_{1-x}Zr_xO_{3-y}$, x = 0.10.

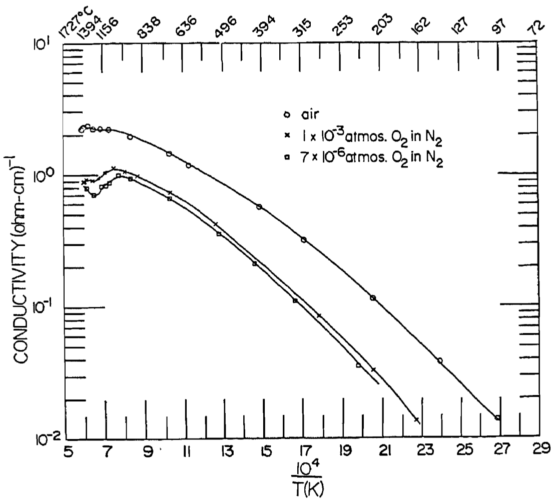

Figure 6B. Electrical conductivity for $[(Y_{0.85}Ca_{0.15})_{1-x}Ca_x]\ Fe_{1-x}Zr_xO_{3-y}$, x = 0.20.

that preparation of powders for fabrication via hot-pressing and, probably, plasma-spraying also should be relatively easy,

b) electrical conductivities are comparable to $LaCrO_3$-based materials,

c) ceramics are not subjected to mechanical damage related to hydration phenomena or to fissuring due to the presence of a secondary phase, and

d) thermal expansion matches magnesia insulation and many leadout-metals.

Disadvantages include,

a) refractoriness, of course, cannot compare with $LaCrO_3$-based materials, especially under highly reducing conditions, and

b) the two-phase nature observed for most materials may compromise corrosion resistance if one of the phases is attacked preferentially.

These disadvantages, however, could be diminished by utilizing these materials as leadouts and/or as "cool" electrodes in a slagging MHD generator.

V. Acknowledgements

We thank T. A. Hahn for the thermal expansion measurements, C. L. McDaniel for the x-ray diffraction work, E. J. Malley for preparative work, and H.P.R. Frederikse for helpful discussions. This work was funded partially by the Department of Energy.

VI. References

1. D. B. Meadowcroft, Brit. J. Appl. Phys. 2, 1225 (1969).

2. See Express Reports (unpublished) by Westinghouse Corp. to Department of Energy for Proof Tests of Phase III, U-02 Candidate Materials, 1977.

3. Personal communication from Dr. M. Yoshimura, 1977.

4. V. I. Strakhov and V. K. Novikov, Zh. Prik. Khim. 48, 2739 (1975).

5. H. J. Van Hook, J. Am. Ceram. Soc. 44, 213 (1961).

6. B. Phillips and A. Muan, J. Am. Ceram. Soc. 41, 448 (1958).

7. W. C. Allen and R. B. Snow, J. Am. Ceram. Soc. 38, 268 (1955).

8. L. H. Brixner, Mat. Res. Bull. 3, 299 (1968).

9. J. B. MacChesney, R. C. Sherwood, and J. F. Potter, J. Chem. Phys. 43, 1907 (1965).